Thin Solid Films 622 (2017) 29–33

Contents lists available at ScienceDirect

Thin Solid Films

journal homepage: www.elsevier.com/locate/tsf

Flexible and high noise margin organic enhancement inverter using hybrid insulator

Dong-Hoon Lee[a], Jinsu Kim[b], Hyeong-Jun Cho[a], Min Su Kim[a], Eung-Kyu Park[a], Nae Eung Lee[b], Yong-Sang Kim[a,*]

[a] The School of Electronics and Electrical Engineering, Sungkyunkwan University, Suwon, Gyeonggi 440-746, South Korea
[b] The SKKU Advanced Institute of Nanotechnology (SAINT), Sungkyunkwan University, Suwon, Gyeonggi 440-746, South Korea

ARTICLE INFO

Article history:
Received 10 May 2016
Received in revised form 28 November 2016
Accepted 28 November 2016
Available online 30 November 2016

Keywords:
Hybrid insulator
Organic thin film transistor
Enhancement inverter
High noise margin

ABSTRACT

We demonstrate a high noise margin and highly flexible enhancement inverter based on the organic-inorganic hybrid insulator. Organic insulators generally show high leakage current and inorganic insulators are brittle. In this work, hybrid insulator was used in pentacene-based organic thin film transistors (OTFTs) to overcome the limitations of each single type of insulator. We report highly flexible OTFTs with reduced threshold voltage and negligible hysteresis using a poly(methyl methacrylate)/silicon nitride hybrid insulator. Using the optimized hybrid insulator, we also demonstrate an enhancement inverter which shows high noise margin with noise margin low of 2.2 V, a noise margin high of 14.1 V and gain of 2.1.

1. Introduction

Exponential growth of flexible electronics technology has allowed people to imagine a large number of innovative products such as electronic paper, wearable displays, radio frequency identification, and disposable medical diagnostic system [1–3]. For this reason, many researchers are studying the device physics of the organic thin film transistor (OTFT), circuit design and synthesizing new organic materials to improve electrical and mechanical performance and reliability [4–6].

A number of novel organic materials have been developed for use as conductor and semiconductor [7]. However, none of the materials has reported a remarkable performance as an insulator. Inorganic materials are brittle and therefore show less flexibility. In contrast, despite their outstanding performance for mechanical bending, organic materials have other limitations such as high leakage current, material instability and low dielectric constant [8,9]. These limitations lead to a high threshold voltage with small noise margins resulting in high power consumption. As most wearable and diagnosis devices adopt a wireless system with a passive type (no battery) power supply [10], organic insulators are not suitable for portable flexible electronics [11]. Therefore, power consumption is an important issue to be resolved.

For these reasons, in this paper, we adopted poly (methyl methacrylate) (PMMA) on silicon nitride (Si_3N_4) as an organic-inorganic stacked hybrid insulator. PMMA is a promising candidate for flexible electronics as it shows negligible hysteresis and excellent electrical performance with a pentacene semiconductor, owing to its hydrophobicity and the presence of carbonyl group in the chemical structure [12–14]. Also, Si_3N_4 is a preferred material for hybrid insulator because of its high dielectric constant, carbon free structure and stability. In addition, it is a commonly used material in the display industry.

The aim of this work is to show the advantages of stacked hybrid insulator in terms of the mechanical and electrical properties, clearly. At first, we evaluated the limitation of organic insulator for the leakage current depending on thickness. Later, we optimized the hybrid insulator by varying its thickness. And the mechanical bending and electrical properties of the hybrid insulator were investigated and compared with single type of insulator. Finally, we demonstrate a p-type enhancement inverter using the hybrid insulator and compare its performance with that of an inverter using single type of organic insulator.

2. Experiment

The bottom gate/top contact structured OTFTs were fabricated with single type of organic and inorganic insulators or hybrid type of organic-inorganic stacked insulator. Fig. 1 shows a schematic of

* Corresponding author.
E-mail address: yongsang@skku.edu (Y. Kim).

http://dx.doi.org/10.1016/j.tsf.2016.11.051
0040-6090/

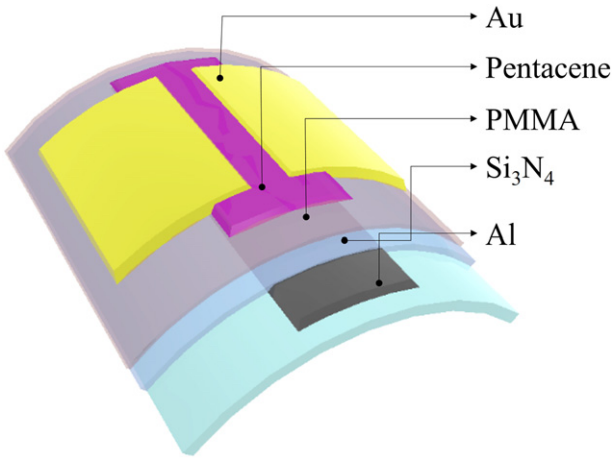

Fig. 1. Schematic of organic TFT using PMMA/Si_3N_4 hybrid insulator.

the OTFT with hybrid insulator on polyethersulfone (PES) plastic substrate. A 100 nm thick aluminum gate electrode was deposited through the shadow mask by thermal evaporation. A Si_3N_4 layer for inorganic insulator was then deposited by plasma enhanced chemical vapor deposition process at a maximum temperature of <200 °C. We used ammonia (NH_3)-free process condition for Si_3N_4 layer due to the low processing temperature and hydrogen concentration. We only used silane and nitrogen gases (gas flow ratio: 1:20) without hydrogen or NH_3 gases at a radio frequency power of 1230 W. PMMA (Sigma, 4 wt.% in toluene) for organic insulator was spin-coated and cured in a conventional oven at 100 °C for 30 min. A pentacene active layer was patterned through the shadow mask by thermal evaporation at a rate of 0.1 Å/s to a thickness of 70 nm. During pentacene deposition, the substrate temperature was fixed at 85 °C. The source and drain electrodes, a 100 nm thick Au layer, were deposited through the shadow mask by thermal evaporation. The electrical measurements were carried out using HP 4145B at room temperature in ambient air.

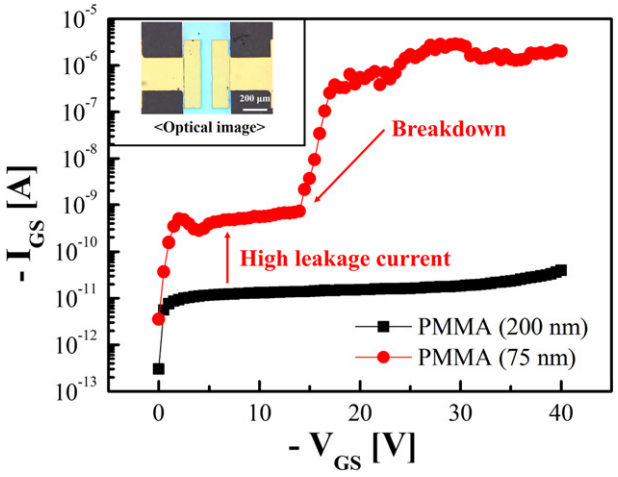

Fig. 2. Gate leakage current of OTFT based on PMMA insulator of 200nm (black) and 75nm (red).

3. Result and discussion

3.1. Limitations of organic insulator

We investigated the gate leakage current of OTFTs with single type of PMMA insulator to show the limitation of organic insulator. Fig. 2 shows the analysis of gate leakage current with different thickness of PMMA insulator (200 and 75 nm). As shown in the inset of Fig. 2, we fabricated the OTFT with length and width of 100 μm and 1000 μm, respectively. Generally, poor step-coverage is one of critical problems of solution-based organic insulator which creates the thin insulator on wall of gate electrode. The solution-based organic insulator shows the limitations such as high gate leakage current and low breakdown voltage by poor step-coverage as shown in Fig. 2. Therefore, organic insulator should be sufficiently thick to prevent the gate leakage current. However, low dielectric constant of organic materials of thick thickness occurs high threshold voltage which limit its use as an insulator in flexible devices.

3.2. Optimization of hybrid insulator

To overcome the limitations of PMMA insulator, we demonstrate a hybrid insulator that incorporates PMMA on Si_3N_4. Fig. 3 (a) and (b) shows the transfer characteristics of OTFTs with hybrid insulator according to insulator thickness. First, we optimized the thickness of PMMA on the Si_3N_4 layer (200 nm), as shown in Fig. 3 (a). The threshold voltage shifted towards positive from −25 to −10 V with the decreasing PMMA thickness. In contrast, the mobility increased slightly due to the smooth surface of insulator. Use of a PMMA layer of

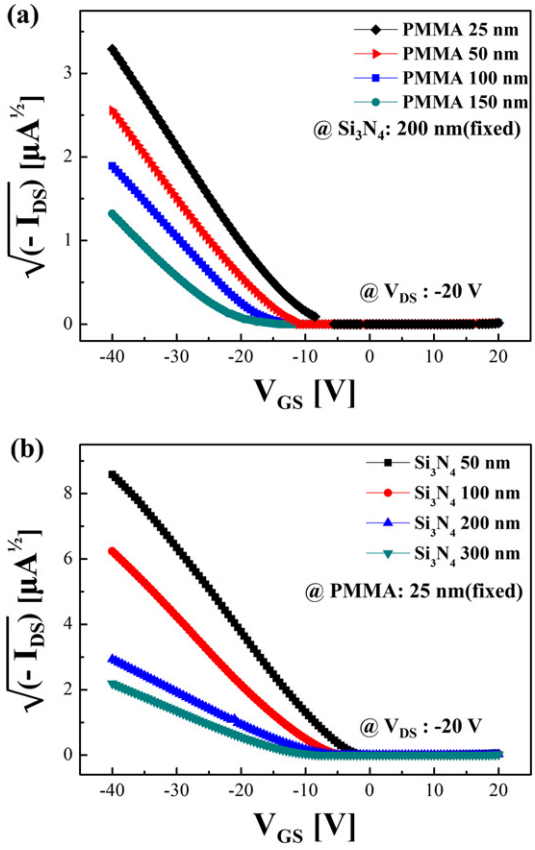

Fig. 3. Transfer characteristic of hybrid insulator-based OTFT with a length of 100 μm and width of 1000 μm for (a) PMMA and (b) Si_3N_4 thickness optimization.

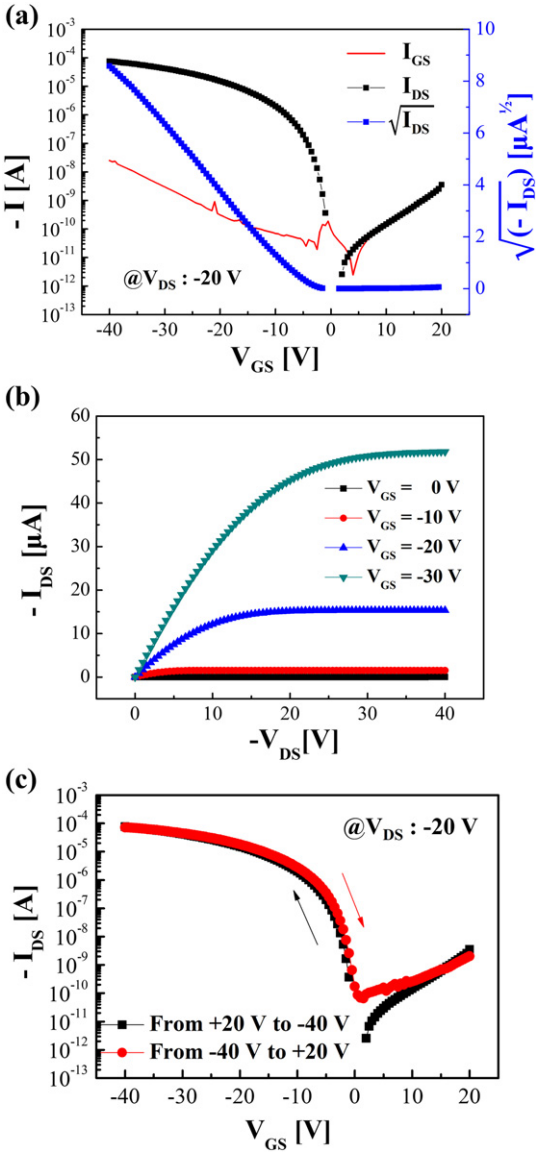

Fig. 4. (a) Output, (b) transfer and (c) hysteresis characteristics of OTFT with the optimized hybrid insulator. The optimized thickness is PMMA and Si_3N_4 of 25 nm and 7 nm, respectively.

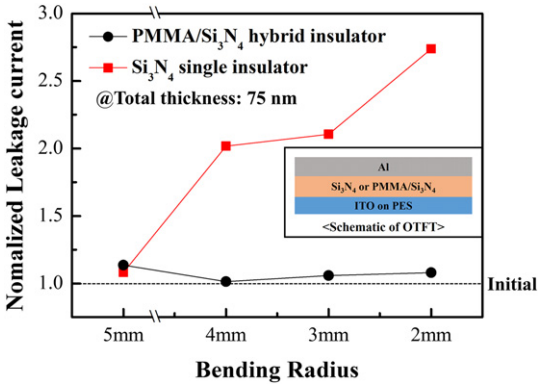

Fig. 5. Comparison of the mechanical bending characteristics of single insulator (black) of PMMA (75 nm) and hybrid insulator (red) of PMMA/Si_3N_4 (25 nm/50 nm) from 5 mm to 2 mm using leakage current analysis of MIM structured device as shown in inset.

<25 nm thickness reduced the device performance. Based on these results, the PMMA thickness was fixed at 20 nm. Next, we optimized the Si_3N_4 thickness using a 25 nm PMMA layer. Fig. 3 (b) shows the transfer characteristics of OTFT with a hybrid insulator according to Si_3N_4 thickness. The hybrid insulator with 50 nm thick Si_3N_4 and 25 nm thick PMMA showed the best performance. A Si_3N_4 layer of <50 nm thickness degraded easily at high voltages. In hybrid configuration, a 50 nm Si_3N_4 layer blocks the gate leakage current. Based on these results, we finalized the hybrid insulator to have PMMA and Si_3N_4 layers of 25 nm and 50 nm thickness, respectively.

3.3. Electrical characteristics of the OTFT using hybrid insulator

We investigated the electrical properties of the OTFT with optimized hybrid insulator. For electrical analysis, we measured the output, transfer and hysteresis characteristics of the OTFT and capacitance of metal-insulator-metal (MIM) structured capacitor to determine the insulating performance.The dielectric constants of PMMA, Si_3N_4 and PMMA on Si_3N_4 insulators are calculated 2.8, 7.0 and 5.2 based on measured capacitance.Fig. 4 shows the output and transfer characteristics of the OTFT with hybrid insulator. As shown in Fig. 4 (b), a negligible gate leakage current exists in the OTFT. The electrical property such as a mobility of the OTFT can be extracted from the transfer characteristics with the following equation:

$$I_{DS(SAT)} = \frac{\mu \cdot W \cdot C_{OX}}{2 \cdot L}(V_G - V_T)^2 \quad (1)$$

The on/off ratio, threshold voltage and mobility were 2.89×10^7, −4.6 V and 0.23 cm^2/V-s, respectively. Also, we investigated the hysteresis of the hybrid insulator as shown in the Fig. 4 (c). The maximum difference in gate voltage (V_{GS}) for a constant current in the forward and reverse scans was designated as the amount of hysteresis (V_H). In our results, the OTFT with hybrid insulator showed a negligible hysteresis behavior of ¡1 V. The solution-based PMMA fills the Si_3N_4 interface avoiding any trap site. Moreover, the hydrophilic surface of Si_3N_4 was covered by the hydrophobic surface

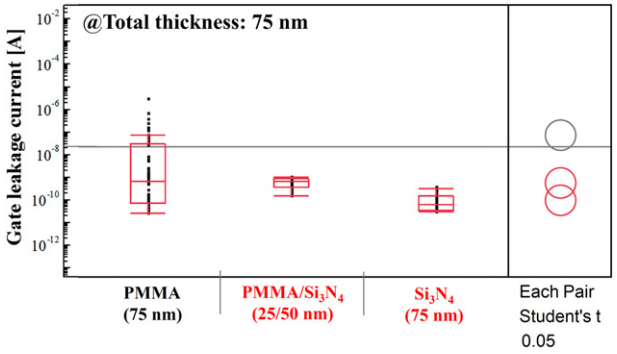

Fig. 6. Comparison of the gate leakage current with single insulator of PMMA and Si_3N_4 and hybrid insulator of PMMA/Si_3N_4.

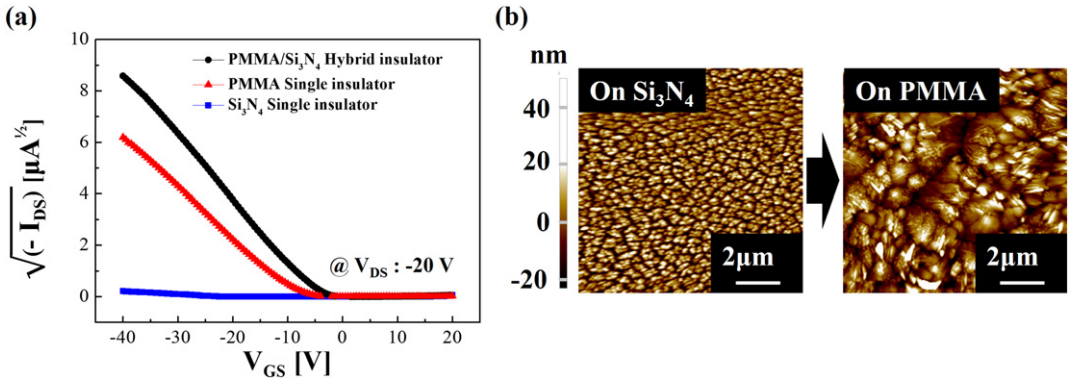

Fig. 7. (a) Comparison of the transfer characteristics with various insulators. (b) AFM images of 70 nm thick pentacene films deposited on Si_3N_4 inorganic insulator and PMMA/Si_3N_4 hybrid insulator.

of PMMA, which is suitable for pentacene deposition. Therefore, an insignificant amount of trap state in the PMMA creates V_H.

3.4. Advantages of the hybrid insulator

3.4.1. Flexibility

To investigate the mechanical bending performance of the OTFT, a MIM structure was fabricated on a PES plastic substrate of 250 μm thickness. We measured the leakage current of the MIM structure with respect to the bending radius of the device, as shown in Fig. 5. The leakage current was normalized to reduce other noise factors. When a mechanical force is applied at the edge to bend the device, tensile and compressive pressure occur on the top and bottom sides of the insulator, respectively. Fig. 5 shows the mechanical bending performance of the hybrid insulator. The leakage current of an single Si_3N_4 layer increased at a bending radius of less than 5 mm. The inorganic insulator such as Si_3N_4 layer alone cannot induce tensile strength due to its brittleness. Therefore, even a small crack increased the leakage current and further bending to a radius smaller than 2 mm extended the crack [15]. Finally, the device breaks down due to capillary cracking following bending to a radius of less than 2 mm. In contrast, the hybrid insulator showed stable leakage current without breakdown until bending to a radius of 2 mm. The solution processing of PMMA prevented capillary cracking of the Si_3N_4 layer, thereby increasing the mechanical stability of the OTFT.

3.4.2. Low gate leakage current

As shown in Fig. 6, the gate leakage current of the PMMA/Si_3N_4 hybrid insulator is compared with single type of PMMA and Si_3N_4 insulators. The thickness of each insulator were equally fixed to 75 nm. The PMMA insulator shows high leakage current. On the other hand, the hybrid insulator and Si_3N_4 single insulator shows low leakage current. The 50 nm thick Si_3N_4 of hybrid insulator can sufficiently block the gate leakage current.

Table 1
Electrical analysis for OTFTs.

	Si_3N_4 insulator	PMMA insulator	Hybrid insulator
Mobility [cm^2/V-s]	8.9×10^{-5}	0.20	0.23
Threshold voltage [V]	−22.7	−10.2	−4.9
On/off ratio	2.20×10^2	1.50×10^7	2.89×10^7
Breaking bending radius [mm]	5	<2	<2
Maximum gate leakage current [A]	2.52×10^{-6}	1.50×10^{-9}	8.9×10^{-10}

3.4.3. Interface compatibility for pentacene growth

We fabricated and compared the electrical performance of OTFTs with single and hybrid type of insulators. The OTFTs were designed with length and width of 100 μm and 1000 μm, respectively. Fig. 7 (a) shows the electrical characteristics of each device with single and hybrid insulators. The Fig. 7 (a) shows the comparison of transfer characteristics and its properties are summarized in Table 1. We measured the atomic-force microscopy (AFM) image of pentacene on the inorganic insulator and hybrid insulator using XE-100 from Park Systems with non-contact mode as shown in Fig. 7 (b). Compared with inorganic insulator, hybrid insulator induced large size of pentacene grain and improved the mobility to 0.23 cm^2/V-s. In addition, hybrid insulator-based OTFT showed a lower threshold voltage than the single organic insulator-based OTFT with similar mobility and on/off ratio.

3.4.4. High noise margin

To demonstrate the feasibility of the flexible and low voltage operable OTFT with hybrid insulator, we used it in the fabrication of an enhancement inverter and measured its electrical performance. The enhancement inverter has a load transistor (TR_L) and drive transistor (TR_D) as shown in the inset of Fig. 8 (a). The enhancement inverter was designed with TR_L of 100 μm/600 μm (length/width) and TR_D of 100 μm/6000 μm. Fig. 8 (a) shows the static voltage transfer characteristics of an enhancement inverter with hybrid insulator compared with those of the PMMA-based single insulator device. The Si_3N_4-based single type inverter without surface treatment was excepted this evaluation due to their lower performance. Table 2 shows the summary of each inverter's characteristic in terms of gain, V_{OH}, V_{OL}, V_{IH}, V_{IL}, noise margin high(NM_H), and noise margin low(NM_L). The noise margin can be calculated from the following equations:

$$NM_H = V_{OH} - V_{IH} \quad (2)$$

$$NM_L = V_{IL} - V_{OL} \quad (3)$$

A higher V_{OH} was obtained because of the lower threshold voltage of hybrid insulator in TR_L. Therefore, the hybrid insulator induced a low voltage drop at the TR_L. Finally, compared to the single insulator type inverter, the PMMA/Si_3N_4 hybrid insulator-based inverter showed a considerably high NM_H as shown in Fig. 8 (b).

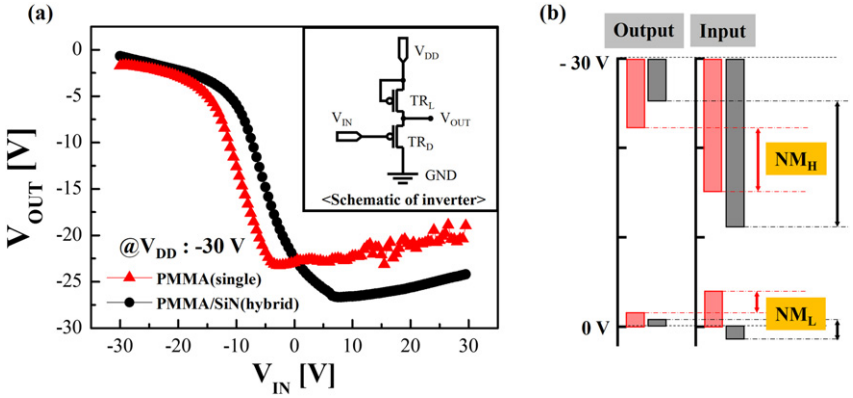

Fig. 8. Comparison of the (a) static voltage transfer characteristics and (b) analysis of static-noise-margin of the enhancement inverter for the two types of insulator.

Table 2
Summary of static voltage transfer characteristics.

Type of insulator	Single insulator	Hybrid insulator
Gain	2.0	2.1
V_{IL} [V]	−4.0	1.6
V_{IH} [V]	−16.1	−12.5
V_{OL} [V]	−1.6	−0.6
V_{OH} [V]	−23.2	−26.6
NM_L [V]	2.4	2.2
NM_H [V]	7.1	14.1

4. Conclusion

A high-performance and flexible OTFT-based on pentacene with an organic-inorganic hybrid insulator was demonstrated. The PMMA/Si_3N_4-based device showed a lower threshold voltage with negligible hysteresis. The device showed no leakage current even after being bent to a radius of 2 mm. Furthermore, the enhancement inverter fabricated using hybrid insulator could be driven with a higher noise margin than a single insulator-based inverter of identical design. Based on these results, a low voltage operated hybrid insulator has several advantages such as low static power due to lower current leakage, and small size due to its higher noise margin and bending property.

References

[1] S. Jeong, D. Kim, S. Lee, B.-K. Park, J. Moon, Organic-inorganic hybrid dielectrics with low leakage current for organic thin-film transistors, Appl. Phys. Lett. 89 (9) (2006) 092101. http://dx.doi.org/10.1063/1.2338753.
[2] S. Shah, J. Smith, J. Stowell, J. Blain Christen, Biosensing platform on a flexible substrate, Sensors Actuators B Chem. 210 (2015) 197–203. http://dx.doi.org/10.1016/j.snb.2014.12.075.
[3] S. Faraji, T. Hashimoto, M.L. Turner, L.A. Majewski, Solution-processed nanocomposite dielectrics for low voltage operated OFETs, Org. Electron. 17 (2015) 178–183. http://dx.doi.org/10.1016/j.orgel.2014.12.010.
[4] S. Jacob, M. Benwadih, J. Bablet, I. Chartier, R. Gwoziecki, S. Abdinia, E. Cantatore, L. Maddiona, F. Tramontana, G. Maiellaro, L. Mariucci, G. Palmisano, R. Coppard, High performance printed N and P-type OTFTs for complementary circuits on plastic substrate, Eur. Solid State Device Res. Conf. (2012) 173–176. http://dx.doi.org/10.1109/ESSDERC.2012.6343361.
[5] L. Wang, M.H. Yoon, A. Facchetti, T.J. Marks, Flexible inorganic/organic hybrid thin-film transistors using all-transparent component materials, Adv. Mater. 19 (20) (2007) 3252–3256. http://dx.doi.org/10.1002/adma.200700393.
[6] T. Umeda, D. Kumaki, S. Tokito, High air stability of threshold voltage on gate bias stress in pentacene TFTs with a hydroxyl-free and amorphous fluoropolymer as gate insulators, Org. Electron.: Phys. Mater. Appl. 9 (4) (2008) 545–549. http://dx.doi.org/10.1016/j.orgel.2008.02.015.
[7] X.-h. Zhang, B. Kippelen, Low-voltage C60 organic field-effect transistors with high mobility and low contact resistance, 93 (2008) (2008) 133305. http://dx.doi.org/10.1063/1.2993349.
[8] S. Yoo, Y.H. Kim, J.-W. Ka, Y.S. Kim, M.H. Yi, K.-S. Jang, Polyimide/polyvinyl alcohol bilayer gate insulator for low-voltage organic thin-film transistors, Org. Electron. 23 (2015) 213–218. http://dx.doi.org/10.1016/j.orgel.2015.05.012.
[9] J.-Y. Oh, S.-C. Lim, J. Yeon Kim, C. Am Kim, K.-I. Cho, S. Deok Ahn, J. Bon Koo, S.-M. Yoon, Organicinorganic hybrid gate dielectric for solution-processed ZnO thin film transistors, J. Vac. Sci. Technol., B: Microelectron. Nanometer Struct. 31 (5) (2013) 050603. http://dx.doi.org/10.1116/1.4817499.
[10] X. Guo, L. Feng, Q. Cui, X. Xu, Low voltage organic/inorganic hybrid complementary inverter with low temperature all solution processed semiconductor and dielectric layers, IEEE Electron Device Lett. 35 (5) (2014) 542–544. http://dx.doi.org/10.1109/LED.2014.2308210.
[11] F.Y. Yang, K.J. Chang, M.Y. Hsu, C.C. Liu, Low-operating-voltage polymeric transistor with solution-processed low-k polymer/high-k metal-oxide bilayer insulators, Org. Electron.: Phys. Mat. Appl. 9 (5) (2008) 925–929. http://dx.doi.org/10.1016/j.orgel.2008.06.002.
[12] D.-H. Lee, J.-M. Kim, J.-W. Lee, Y.-S. Kim, Improved organic rectifier using polymethyl-methacrylate-poly 4-vinylphenol double layer, Micro Nano Lett. 6 (7) (2011) 567–570. http://dx.doi.org/10.1049/mnl.2011.0094.
[13] X. Hou, S.C. Ng, J. Zhang, J.S. Chang, Polymer nanocomposite dielectric based on P(VDF-TrFE)/PMMA/$BaTiO_3$ for TIPs-pentacene OFETs, Org. Electron. 17 (2015) 247–252. http://dx.doi.org/10.1016/j.orgel.2014.12.012.
[14] Y. Wang, H. Kim, UV-curable organicinorganic hybrid gate dielectrics for organic thin film transistors, Organic Electronics 13 (12) (2012) 2997–3003. http://dx.doi.org/10.1016/j.orgel.2012.08.014.
[15] B.-U. Hwang, D.-I. Kim, S.-W. Cho, M.-G. Yun, H.J. Kim, Y.J. Kim, H.-K. Cho, N.-E. Lee, Role of ultrathin Al_2O_3 layer in organic/inorganic hybrid gate dielectrics for flexibility improvement of InGaZnO thin film transistors, Org. Electron. 15 (7) (2014) 1458–1464. http://dx.doi.org/10.1016/j.orgel.2014.04.003.